JOC Article

Chromatographic Resolution, Solution and Crystal Phase Conformations, and Absolute Configuration of *tert*-Butyl(dimethylamino)phenylphosphine−Borane Complex

Jean-Valère Naubron,[†] Laurent Giordano,[†] Frédéric Fotiadu,*[,†] Thomas Bürgi,[‡] Nicolas Vanthuyne,[†] Christian Roussel,[†] and Gérard Buono*[,†]

UMR 6180 CNRS: "Chirotechnologies: Catalyse et Biocatalyse", Université Paul Cézanne, EGIM, Avenue Escadrille Normandie-Niémen, 13397 Marseille Cedex 20, France, and Université de Neuchâtel, Institut de Chimie, Avenue Bellevaux 51, CH-2007 Neuchâtel, Switzerland

frederic.fotiadu@egim-mrs.fr; gerard.buono@egim-mrs.fr.

Received March 14, 2006

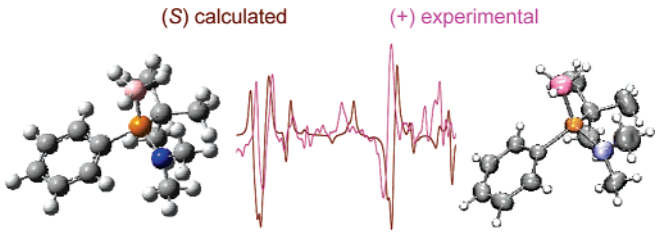

The enantiomers of *tert*-butyl(dimethylamino)phenylphosphine−borane complex **2** have been separated by HPLC using cellulose tris-*p*-methylbenzoate as chiral stationary phase. The borane protection could be removed without racemization and the P-configuration of the free aminophosphine **1** has shown to be stable in solution. Infrared (IR) and vibrational circular dichroism (VCD) spectra have been measured in CD_2Cl_2 solution for both enantiomers. B3LYP/6-31+G(d) DFT calculations allowed a prediction that complex (*S*)-**2** exists as three conformers in equilibrium and computed population-weighted IR and VCD spectra. Predicted and experimental IR and VCD spectra compared very well and indicate that enantiomer (+)-**2** has the *S* absolute configuration. This assignment has been confirmed by an X-ray diffraction study on a single crystal of (+)-**2**. The crystal structure of enantiomerically pure **2** appears to be very close to the most stable computed conformer which proved to be predominant in solution.

Introduction

Chiral tricoordinated organophosphorus ligands play a central role in the development of asymmetric homogeneous catalysis.[1] Among these, a number of phosphine derivatives containing a P−N bond have been described and successfully applied in stereoselective catalysts.[2] Most of these ligands bear chirality on their organic moiety and not at the phosphorus center. Such ligands are usually prepared by exchange reactions between a chiral amine and a chlorophosphine or a dialkylaminophosphine as a trivalent phosphorus precursor.[2,3] Diastereomerically pure aminophosphine derivatives bearing also chirality at the phosphorus atom have been obtained in a similar way via highly diastereoselective exchange reactions, in which chirality is transmitted from amine to phosphorus.[4−6] However, literature offers very rare examples of enantiomerically pure aminophosphines with the phosphorus atom as the single chirogenic center. In their pioneering works, Horner and Jordan prepared enantiomerically enriched diethylaminoethylphenylphosphine by

[†] CNRS.
[‡] Institut de Chimie.

(1) (a) Brunner, H.; Zettlmeier, W. *Handbook of Enantioselective Catalysis with Transition Metal Compounds, Ligands-References*; VCH: Basel, Switzerland, 1993; Vol. 2. (b) Noyori, R. *Asymmetric Catalysis in Organic Synthesis*; Wiley & Sons: New York, 1994. (c) *Comprehensive Asymmetric Catalysis*; Jacobsen, E. N., Pfaltz, A., Yamamoto, H., Eds.; Springer-Verlag: Berlin, 1999. (d) *Catalytic Asymmetric Synthesis*; Ojima, I., Ed.; Wiley-VCH: New York, 2000. For a pertinent review on monophosphine ligands, see the following: (e) Lagasse, F.; Kagan, H. B. *Chem. Pharm. Bull.* **2000**, *48*, 315−324. (f) Komarov, I. V.; Börner, A. *Angew. Chem., Int. Ed.* **2001**, *40*, 1197−1200. (g) Tang, W.; Zhang, X. *Chem. Rev.* **2003**, *103*, 3029−3069. (h) Valentine, D. H., Jr.; Hillhouse, J. H. *Synthesis* **2003**, *16*, 2437−2460. (i) Jerphagnon, T.; Renaud, J.-L.; Bruneau, C. *Tetrahedron: Asymmetry* **2004**, *15*, 2101−2111.

(2) See for instances: (a) Petit, M.; Mortreux, A.; Petit, F.; Buono, G.; Peiffer, G. *New J. Chem.* **1983**, *7*, 593−596 (b) Buono, G.; Siv, C.; Peiffer, G.; Triantaphylides, C.; Denis, P.; Mortreux, A.; Petit, F. *J. Org. Chem.* **1985**, *50*, 1781−1782. (c) Mortreux, A.; Petit, F.; Buono, G.; Peiffer, G. *Bull. Soc. Chim. Fr.* **1987**, 631−639. (d) Agbossou, F.; Carpentier, J. F.; Hapiot, F.; Suisse, I.; Mortreux, A. *Coord. Chem. Rev.* **1998**, 178−180, 1615−1645. (e) Dyer, P. W.; Fawcett, J.; Hanton, M. J.; Kemmitt, R. D. W.; Padda, R.; Singh, N. *J. Chem. Soc., Dalton Trans.* **2003**, 104−113.

(3) Quin, L. D. *A Guide to Organophosphorus Chemistry*; Wiley-Interscience: New York, 2000.

10.1021/jo0605647 CCC: $33.50
Published on Web 06/20/2006

electrochemical reduction or cyanolysis of the corresponding resolved amidophosphonium salts.[7] These phosphinous amides proved to be configurationally stable but very sensitive to oxidation. Our current research project required enantiopure samples of both antipodes of a P-chirogenic aminophosphine of known absolute configuration. We focused on *tert*-butyl-(dimethylamino)phenylphosphine **1**, for which racemic alkylamino and dialkylamino analogues have been described.[8] Several diastereomeric alkylamino-*tert*-butylphenylphosphines related to **1** deriving from a chiral amine moiety have also been reported.[4] Absolute configuration at the phosphorus atom has been deduced from the known configuration of the amine moiety and the relative stereochemistry that could be assigned either from NMR studies or X-ray diffraction of the crystallized phosphine or its borane adduct.[4,5,9] In the case of P-chiral compounds related to aminophosphine **1**, absolute configurations have been deduced from chemical correlation with phosphorus derivatives of known stereochemistry.[10] Recently, Polavarapu et al. have used vibrational circular dichroism (VCD) spectroscopy in conjunction with density functional theory (DFT) calculations to determine the predominant conformation and phosphorus absolute configuration of *tert*-butylphenylphosphine oxide,[11] *tert*-butyl-1-(2-methylnaphthyl)phosphine oxide,[12] *tert*-butylphenylphosphinothioic acid,[13] and *tert*-butylphenylphosphinoselenoic acid,[14] which are pentavalent phosphorus compounds structurally close to **1**. During the last years, VCD has emerged as a technique of choice to assign absolute configuration to chiral compounds and elucidate their conformational equilibriums.[15] The implementation of quantum mechanical methods that provide reliable predictions of VCD spectra in commercial quantum chemistry packages[16] made application of this technique more straightforward.[17] General methodology consists, first, to identify the stable conformations of a chiral molecule, second, to compute theoretical spectra for each individual conformer and deduce the population-averaged VCD spectra for each enantiomer, and third, to compare these spectra with the experimental record for an enantiopure or enantiomerically enriched sample in solution.[11−15] As far as we know, this approach has not been previously applied to trivalent phosphorus compounds.[18]

In this work, we apply such a combination of DFT calculations and VCD measurements to assign absolute configuration to the enantiomers of borane adduct **2** of aminophosphine **1**. Borane protection prevents oxidation of trivalent phosphorus species **1** and allows easier manipulation and storage.[19] Chiral liquid chromatography contribution to the determination of the

(4) For diastereoselectivity induced by chiral amines see the following: (a) Kolodiazhnyi, O. I.; Gryshkun, E. V.; Andrushko, N. V.; Freytag, M.; Jones, P. G.; Schmutzler, R. *Tetrahedron: Asymmetry* **2003**, *14*, 181−184. (b) Gryshkun, E. V.; Andrushko, N. V.; Kolodiazhnyi, O. I. *Phosphorus, Sulfur Silicon Relat. Elem.* **2004**, *179*, 1027−1046.

(5) For diastereoselectivity induced by chiral diamines, amino alcohols, or related compounds see the following: (a) Jugé, S.; Stephan, M.; Laffitte, J. A.; Genêt, J. P. *Tetrahedron Lett.* **1990**, *31*, 6357−6360. (b) Jugé, S.; Stephan, M.; Achi, S.; Genêt, J. P. *Phosphorus, Sulfur, Silicon Relat. Elem.* **1990**, *49/50*, 267−270. (c) Buono, G.; Brunel, J. M.; Faure, B.; Pardigon, O. *Phosphorus, Sulfur Silicon Relat. Elem.* **1993**, *75*, 43−46. (d) Jugé, S.; Stephan, M.; Merdès, R.; Genêt, J. P.; Halut-Desportes, S. J. *J. Chem. Soc., Chem. Commun.* **1993**, 531−533. (e) Chiodi, O.; Fotiadu, F.; Sylvestre, M.; Buono, G. *Tetrahedron Lett.* **1996**, *37*, 39−42. (f) Brunel, J. M.; Constantieux, T.; Buono, G. *J. Org. Chem.* **1999**, *64*, 8940−8942. (g) Breeden, S.; Wills, M. *J. Org. Chem.* **1999**, *64*, 9735−9738. (h) Legrand, O.; Brunel, J. M.; Buono, G. *Angew. Chem., Int. Ed.* **1999**, *38*, 1479−1483. (i) Brunel, J. M.; Legrand, O.; Reymond, S.; Buono, G. *J. Am. Chem. Soc.* **1999**, *121*, 5807−5808. (j) Moulin, D.; Darcel, C.; Jugé, S. *Tetrahedron: Asymmetry* **1999**, *10*, 4729−4743. (k) Ngono, C. J.; Constantieux, T.; Buono, G. *J. Organomet. Chem.* **2002**, *643−644*, 237−246. (l) Delapierre, G.; Achard, M.; Buono, G. *Tetrahedron Lett.* **2002**, *43*, 4025−4028. (m) Bauduin, C.; Moulin, D.; Kaloun, E. B.; Darcel, C.; Jugé, S. *J. Org. Chem.* **2003**, *68*, 4293−4301. (n) Hersh, W. H.; Xu, P.; Simpson, C. K.; Grob, J.; Bickford, B.; Hamdani, M. S.; Wood, T.; Rheingold, A. L. *J. Org. Chem.* **2004**, *69*, 2153−2163.

(6) Crepy, K. V. L.; Imamoto, T. *Top. Curr. Chem.* **2003**, *229*, 1−40.

(7) (a) Horner, L.; Jordan, M. *Phosphorus Sulfur* **1980**, *8*, 225−234. (b) Horner, L.; Jordan, M. *Phosphorus Sulfur* **1980**, *8*, 235−242. (c) Horner, L. *Pure Appl. Chem.* **1980**, *52*, 843−858. (c) For the preparation of the enantiomers of compounds containing chiral phosphorus centres see the following: Valentine, D., Jr. *Asymmetric Synthesis*; Morrison, J. D.; Scott, J. W. Eds.; Academic Press: New York, 1984; Vol. 4, pp 263−312.

(8) (a) Gruber, M.; Schmutzler, R. *Phosphorus, Sulfur Silicon Relat. Elem.* **1993**, *80*, 181−194. (b) Maier, L.; Diel, P. J. *Phosphorus, Sulfur Silicon Relat. Elem.* **1996**, *115*, 273−300.

(9) Jugé, S.; Stephan, M.; Genêt, J. P.; Halut-Desportes, S.; Jeannin, S. *Acta Crystallogr., Sect. C: Cryst. Struct. Commun.* **1990**, *C46*, 1969−1872.

(10) (a) Horner, L.; Jordan, M. *Phosphorus Sulfur* **1979**, *6*, 491−493. (b) Mikolajczyk, M.; Omelanczuk, J.; Perlikowska, W. *Tetrahedron* **1979**, *35*, 1531−1536. (c) Mikolajczyk, M. *Pure Appl. Chem.* **1980**, *52*, 959−972.

(11) Wang, F.; Polavarapu, P. L.; Drabowicz, J.; Mikolajczyk, M. *J. Org. Chem.* **2000**, *65*, 7561−7565.

(12) Wang, F.; Wang, Y.; Polavarapu, P. L.; Li, T.; Drabowicz, J.; Pietrusiewicz, K. M.; Zygo, K. *J. Org. Chem.* **2002**, *67*, 6539−6541.

(13) Wang, F.; Polavarapu, P. L.; Drabowicz, J.; Mikolajczyk, M.; Lyzwa, P. *J. Org. Chem.* **2001**, *66*, 9015−9019.

(14) Wang, F.; Polavarapu, P. L.; Drabowicz, J.; Kielbasinski, P.; Potrzebowski, M. J.; Mikolajczyk, M.; Wieczorek, M. W.; Majzner, W. W.; Lazewska, I. *J. Phys. Chem. A* **2004**, *108*, 2072−2079.

(15) (a) Stephens, P. J.; Devlin, F. J. *Chirality* **2000**, *12*, 172−179. (b) Devlin, F. J.; Stephens, P. J.; Scafato, P.; Superchi, S.; Rosini, C. *Chirality* **2002**, *14*, 400−406. (c) Solladie-Cavallo, A.; Marsol, C.; Yaakoub, M.; Azyat, K.; Klein, A.; Roje, M.; Suteu, C.; Freedman, T. B.; Cao, X.; Nafie, L. A.; *J. Org. Chem.* **2003**, *68*, 7308−7315. (d) Herse, C.; Bas, D.; Krebs, F. C.; Bürgi, T.; Weber, J.; Wesolowski, T.; Laursen, B. W.; Lacour, J. *Angew. Chem., Int. Ed.* **2003**, *42*, 3162−3166. (e) Bürgi, T.; Urakawa, A.; Behzadi, B.; Ernst, K.-H.; Baiker, A. *New J. Chem.* **2004**, *28*, 332−334. (f) He, J. T.; Petrovich, A.; Polavarapu, P. L. *J. Phys. Chem. A* **2004**, *108*, 1671−1680. (g) Nafie, L. A. *J. Phys. Chem. A* **2004**, *108*, 7222−7231. (h) Taniguchi, T.; Miura, N.; Nishimura, S.-I.; Monde, K. *Mol. Nutr. Food Res.* **2004**, *48*, 246−254. (i) Cerè, V.; Peri, F.; Pollicino, S.; Ricci, A.; Devlin, F. J.; Stephens, P. J.; Gasparrini, F.; Rompietti, R.; Villani, C. *J. Org. Chem.* **2005**, *70*, 664−669. (j) Devlin, F. J.; Stephens, P. J.; Besse, P. *J. Org. Chem.* **2005**, *70*, 2980−2993.

(16) Frisch, M. J.; Trucks, G. W.; Schlegel, H. B.; Scuseria, G. E.; Robb, M. A.; Cheeseman, J. R.; Montgomery, J. A., Jr.; Vreven, T.; Kudin, K. N.; Burant, J. C.; Millam, J. M.; Iyengar, S. S.; Tomasi, J.; Barone, V.; Mennucci, B.; Cossi, M.; Scalmani, G.; Rega, N.; Petersson, G. A.; Nakatsuji, H.; Hada, M.; Ehara, M.; Toyota, K.; Fukuda, R.; Hasegawa, J.; Ishida, M.; Nakajima, T.; Honda, Y.; Kitao, O.; Nakai, H.; Klene, M.; Li, X.; Knox, J. E.; Hratchian, H. P.; Cross, J. B.; Bakken, V.; Adamo, C.; Jaramillo, J.; Gomperts, R.; Stratmann, R. E.; Yazyev, O.; Austin, A. J.; Cammi, R.; Pomelli, C.; Ochterski, J. W.; Ayala, P. Y.; Morokuma, K.; Voth, G. A.; Salvador, P.; Dannenberg, J. J.; Zakrzewski, V. G.; Dapprich, S.; Daniels, A. D.; Strain, M. C.; Farkas, O.; Malick, D. K.; Rabuck, A. D.; Raghavachari, K.; Foresman, J. B.; Ortiz, J. V.; Cui, Q.; Baboul, A. G.; Clifford, S.; Cioslowski, J.; Stefanov, B. B.; Liu, G.; Liashenko, A.; Piskorz, P.; Komaromi, I.; Martin, R. L.; Fox, D. J.; Keith, T.; Al-Laham, M. A.; Peng, C. Y.; Nanayakkara, A.; Challacombe, M.; Gill, P. M. W.; Johnson, B.; Chen, W.; Wong, M. W.; Gonzalez, C.; Pople, J. A. *Gaussian 03*, revision B.03; Gaussian, Inc.: Wallingford, CT, 2004.

(17) (a) Cheeseman, J. R.; Frisch, M. J.; Devlin, F. J.; Stephens, P. J. *Chem. Phys. Lett.* **1996**, *252*, 211−220. (b) Devlin, F. J.; Stephens, P. J.; Cheeseman, J. R.; Frisch, M. J. *J. Phys. Chem. A.* **1997**, *101*, 9912−9924.

(18) Polavarapu et al. have shown that, although *tert*-butylphenylphosphine oxide and *tert*-butyl-1-(2-methylnaphthyl)phosphine oxide can exist in an equilibrium between pentavalent and trivalent tautomeric structures, only one pentavalent (tetracoordinated P) form is present in solution.[11,12]

(19) The synthesis of phosphines has been extremely simplified by their protection as phosphine−borane complexes, which are inert to moisture and air: (a) Imamoto, T. *Pure Appl. Chem.* **1993**, *65*, 655−660. (b) Brunel, J. M.; Faure, B.; Maffei, M. *Coord. Chem. Rev.* **1998**, *178−180*, 665−698. (c) Ohff, M.; Holz, J.; Quirmbach, M.; Börner, A. *Synthesis* **1998**, 1391−1415. (d) Carboni, B.; Monnier, L. *Tetrahedron* **1999**, *55*, 1197−1248. (e) Darcel, C.; Kaloun, E. B.; Merdès, R.; Moulin, D.; Riegel, N.; Thorimbert, S.; Genêt, J. P.; Jugé, S. *J. Organomet. Chem.* **2001**, *624*, 333−343. (f) Maienza, F.; Spindler, F.; Thommen, M.; Pugin, B.; Malan, C.; Mezzetti, A. *J. Org. Chem.* **2002**, *67*, 5239−5249. See also Moulin et al.[5j]

SCHEME 1

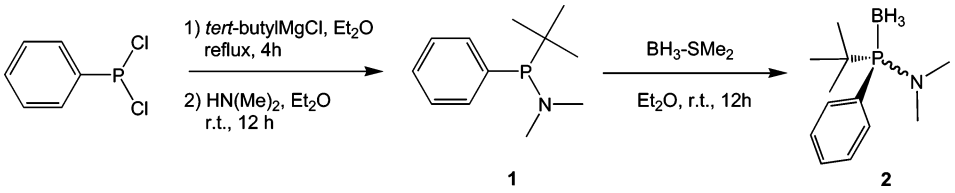

absolute configuration of enantiomers have recently been reviewed by Roussel et al.[20] Preparative chiral HPLC combined with physicochemical methods is a powerful tool to determine absolute configuration: chiral chromatography provides pure enantiomers and then the absolute configuration of an isolated enantiomer can be assigned by X-ray analysis, VCD, NMR, optical rotation, or CD. A systematic screening procedure of commercially available chiral columns with an automated HPLC system allows finding suitable conditions for resolution of complex **2** on a semipreparative scale. From a comparison between experimental infrared (IR) and VCD spectra and theoretical predictions, the three conformers of **2** present in solution are identified. The structure of (+)-*tert*-butyl(dimethylamino)phenylphosphine−borane **2** in the solid phase is obtained from single-crystal X-ray diffraction and corresponds to the most stable conformation in solution. Finally, assignment of the absolute configuration is confirmed by the X-ray studies.

Results and discussion

Following a procedure similar to that used by Maier,[8b] racemic phosphine−borane **2** was readily prepared from dichlorophenylphosphine in a three steps one-pot reaction sequence (Scheme 1). $PhPCl_2$ was first allowed to react with 3 equiv of *tert*-butylmagnesium chloride in ether, then with a large excess of dimethylamine, to give *tert*-butyl(dimethylamino)phenylphosphine **1** that has not been isolated. Reactions were monitored by ^{31}P NMR spectroscopy, total conversion at each step being confirmed by a single signal at 121.9 ppm for intermediate *tert*-butylchlorophenylphosphine, then 85.4 ppm for aminophosphine **1**. Further protection of **1** with BH_3-SMe_2 afforded *rac*-**2** in 31% overall yield from starting material after chromatographic purification (δ ^{31}P = 87.8 ppm). Complex **2** was air and moisture stable, soluble and inert in common alkane, chloroalkane, methanol, and aromatic solvents. This prompted us to intent to resolve *rac*-**2** by liquid chromatography on chiral stationary phase. The enantiomers of a number of racemic organophosphorus compounds have been separated by chiral HPLC. However, according to Chirbase database, no chiral HPLC resolution of trivalent phosphorus compound including a P−N bond, either free or as its borane adduct, has been reported in the literature.[21] Therefore, a screening procedure of 11 commercially available chiral stationary phases was applied to find suitable analytical chromatographic conditions for phosphine−borane complex **2**. It resulted that only cellulose tris-*p*-methylbenzoate (Chiralcel OJ-H) with hexane/propan-2-ol 99/1 as the eluent was able to separate the enantiomers. The chromatographic method developed was scaled-up with a semipreparative Chiralcel OJ (250 × 10 mm) column. Iterative injections afforded ca. 30 mg of each enantiomer with ee > 99% in 1 h.

Decomplexation of a sample of enantiopure dextrorotatory borane complex **2** was achieved by heating the sample at 45 °C with DABCO; then the free aminophosphine **1** was purified by filtration through activated neutral alumina and characterized by ^{31}P NMR spectroscopy. A new protection of this free aminophosphine was achieved with BH_3-SMe_2. The enantiomeric purity of the resulting complex (+)-**2** was the same as before de- and reprotection (>99% ee by chromatographic analysis). This indicates that no epimerization occurs upon de- and reprotection and that the P-configuration of the free aminophosphine **1** is stable in solution under the chemical and thermal conditions we used. This opens the way to applications of enantiopure aminophosphine **1** in asymmetric synthesis or catalysis. It is worth noting that borane complex (+)-**2** might also be used directly as a pro-ligand for transition metal catalyzed reactions, according to a recently reported procedure.[19f]

DFT calculations and VCD spectroscopy were performed to establish the absolute configuration at the phosphorus atom of resolved (+) and (−)-**2**. Conformational analysis of (*S*)-**2** at the B3LYP/6-31+G(d) level was carried out by rotating simultaneously the phenyl and dimethylamino groups and allowing full relaxation of the rest of the structure. Because of steric hindrance around the tetracoordinated phosphorus center, one group could not be rotated independently of the other and collapse of the substituents occurred during conformational exploration. Careful scanning of the potential energy surface by varying the C_7C_2-PB and C_{14}NPB dihedral angles (Figure 1) allowed us to find three distinct minima.[22] The corresponding fully optimized geometries are depicted in Figure 1. The converged dihedral angles, optimized electronic energies, Gibbs energies, and relative populations are listed in Table 1. For the three structures, the P−*t*-Bu and P−BH_3 bonds exhibit slightly distorted staggered conformations, as one can expect. In the highest energy conformer **a**, the phenyl ring is nearly eclipsed with the P−B bond, whereas it is almost perpendicular in the most stable form **c**. In both cases, the dimethylamino group exhibits a synclinal orientation with respect to the P−B bond. The pyramidalization of the nitrogen atom, which is measured by the $C_{14}NPC_{13}$ dihedral angle (Figure 1), is affected by the rotation of the phenyl ring. Probably because of strong steric repulsions with the proximal ortho position of the phenyl ring, the NMe_2 group tends to adopt a more flattened geometry in conformation **c** compared to **a** ($C_{14}NPC_{13}$ = 158.6° instead of 143.8°). Completely different orientations of the two rotatable substituents were encountered in conformer **b**: the phenyl ring is

(20) Roussel, C.; Del Rio, A.; Pierrot-Sanders, J.; Piras, P.; Vanthuyne, N. *J. Chromatogr. A* **2004**, *1037*, 311−328.

(21) (a) Roussel, C.; Piras, P. *Pure Appl. Chem.* **1993**, *65*, 235−244. (b) Roussel, C.; Pierrot-Sanders, J.; Hietmann, I.; Piras, P. CHIRBASE, Database current status and derived research applications using molecular similarity, decision tree and 3D ≪ enantiophore ≫ search. In *Chiral Separation Techniques − A Practical Approach*, 2nd ed.; Subramanian, G., Ed.; Wiley-VCH: Weinheim, Germany, 2001; pp 95−125.

(22) Because of the local C_2 symmetry of the phenyl ring and the possibility of inverting the nitrogen atom of the dimethylamino group during potential energy surface exploration, redundant structures having the same energy could be located. Only the three distinct stable conformations are presented here.

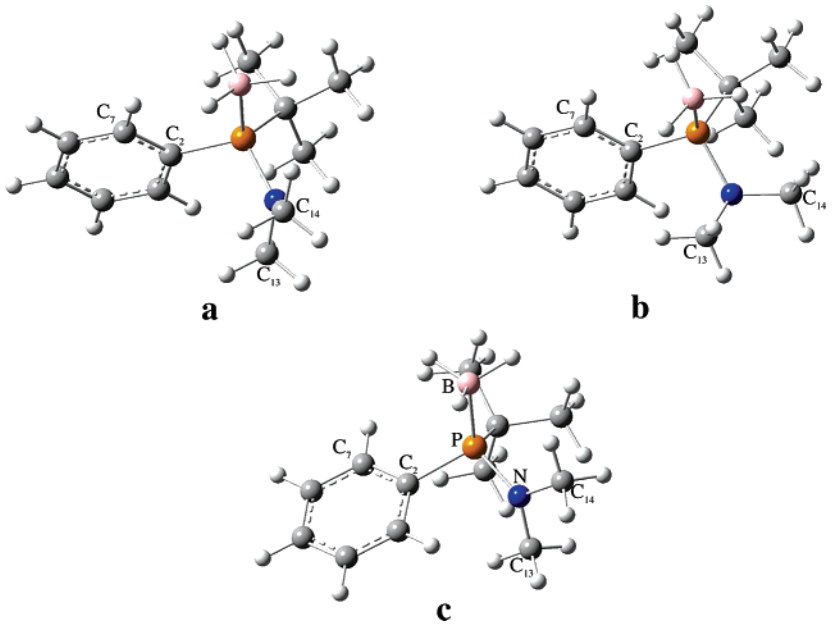

FIGURE 1. Optimized B3LYP/6-31+G(d) structures of the three stable conformations **a**, **b**, and **c** of (*S*)-*tert*-butyl(dimethylamino)phenylphosphine−borane and atom numbering used to define characteristic dihedral angles.

TABLE 1. Conformations and B3LYP/6-31+G(d) Energies of (*S*)- *tert*-Butyl(dimethylamino)phenylphosphine−Borane

	dihedral angles[a]			energy[b]			
conformer[a]	C_2C_7PB	$C_{14}NPB$	$C_{14}NPC_{13}$	electronic	Gibbs	ΔG^c (kcal mol^{-1})	population[d] (%)
a	5.5	−14.7	143.8	−892.09850	−891.81231	1.12	10.8
b	20.1	59.8	129.1	−892.09921	−891.81281	0.81	18.2
c	78.0	−22.4	158.6	−892.09957	−891.81410	0.00	71.0

[a] See Figure 1 for labels, angles in degree. [b] In hartrees. [c] Relative Gibbs energy difference in kcal mol^{-1}. [d] Population at 298 K based on Gibbs energies.

synclinal, having an intermediate torsion between the ones in **a** and **c**, and the dimethylamino group adopts a local C_s symmetry with respect to P−BH_3. In this orientation, the nitrogen atom presents a rigorously pyramidal arrangement, with 129.1° for the $C_{14}NPC_{13}$ angle. Because of their antiperiplanar orientation, a strong overlap between the nitrogen lone pair of electrons and the P−B bond (i.e., negative hyperconjugation) should explain this nitrogen sp^3 type hydridization in conformer **b**.[23] The two different orientations of the NMe_2 group observed in conformer **a** and **c** on one hand, and **b** on the other hand, are reminiscent of previous findings concerning the geometry of tris(dimethylamino)phosphoranes, $(Me_2N)_3P-BH_3$,[24] and more generally $P(NR_2)_3$ skeletons and related fragments.[25] In such compounds, dialkylamino groups of two different coordination geometries similar to what we found (either synclinal with a flattened nitrogen environment or local C_s symmetry with a pyramidal nitrogen environment) coexist in the same molecule as the result of electronic effects. Contrary to previously studied tetracoordinated phosphorus species bearing *tert*-butyl and aryl substituents,[11−14] the preferred conformation of complex **2** does not correspond to a nearly perpendicular arrangement of the phenyl ring with respect to the bulky *tert*-butyl group, as observed in conformer **b**. Instead, conformer **c** in which the phenyl ring is synclinal with respect to P−*t*-Bu and perpendicular to P−BH_3 is slightly more stable than **b** and **a**. However, the energies of conformers **a**, **b**, and **c** are very similar, spanning a range of 1.12 kcal mol^{-1}. Furthermore, the computed barriers to internal rotations are very low: for instance, the transition state allowing the conversion of conformer **a** into **b** is only 2.45 kcal mol^{-1} (see Supporting Information). Therefore, (*S*)-**2** is predicted to exist as an equilibrium mixture of all three conformations at 298 K. The equilibrium populations were calculated from Gibbs energies for isolated molecules using Boltzmann statistics (Table 1). Although conformer **c** is predominant (71%), the alternative allowed conformations of (*S*)-**2** **a** and **b**, are predicted to be significantly populated.

The IR and VCD intensities were calculated for the three conformers at the B3LYP/6-31+G(d) level. In each case, the most intense bands correspond to B−H stretching in the 2300−2400 cm^{-1} region. For instance, dissymmetric and symmetric B−H stretching bands appear at 2415 (no. 1) and 2363 (no. 2) cm^{-1}, respectively, for conformer **c**. Calculations predict that the corresponding VCD signals are relatively intense and present characteristic positive-negative alternations which are isolated from others bands of the spectra (see Supporting Information). Therefore, these signals could have been of great interest to assign absolute configuration to complex **2**, and from a more general point of view, to any phosphine−borane adduct that should present similar bands. Unfortunately, we could not obtain satisfactorily experimental spectra in this region because of poorer signal-to-noise ratio above 1800 cm^{-1},[26] overlap with

(23) Gilheany, D. G. *Chem. Rev.* **1994**, *94*, 1339−1374.
(24) Mitzel, N. W.; Lustig, C. *J. Chem. Soc., Dalton Trans.* **1999**, 3177−3183.
(25) (a) Mitzel, N. W.; Smart, B. A.; Dreihäupl, K.-H.; Rankin, D. W. H.; Schmidbaur, H. *J. Am. Chem. Soc.* **1996**, *118*, 12673−12682. (b) Belyakov, A. V.; Baskakova, P. E.; Haaland, A.; Swang, O.; Bilkov, L. V.; Bolubinskii, A. V.; Bogoradovskii, E. T. *Russ. J. Gen. Chem.* **1998**, *68*, 244−250.

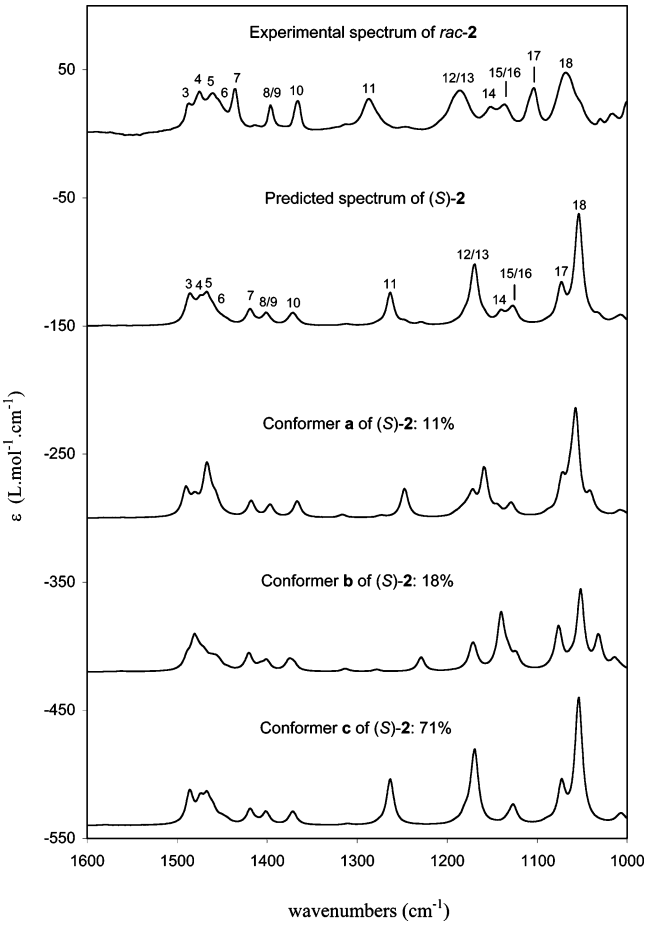

FIGURE 2. Comparison of the experimental IR spectrum of *tert*-butyl(dimethylamino)phenylphosphine−borane **2** at 0.06 M in CD_2Cl_2 solution (top trace) with predicted IR spectra (bottom three traces) of stable conformations of the *S* configuration (structure and conformation labels in Figure 1) obtained with the B3LYP/6-31+G(d) level. For predicted spectra, wavenumbers are scaled by the factor 0.9614. The trace labeled "predicted" (second from top) is the population-weighted spectrum with populations given in Table 1. Numbers indicate corresponding features in the predicted spectrum of (*S*)-**2** and the experimental spectrum of **2**.

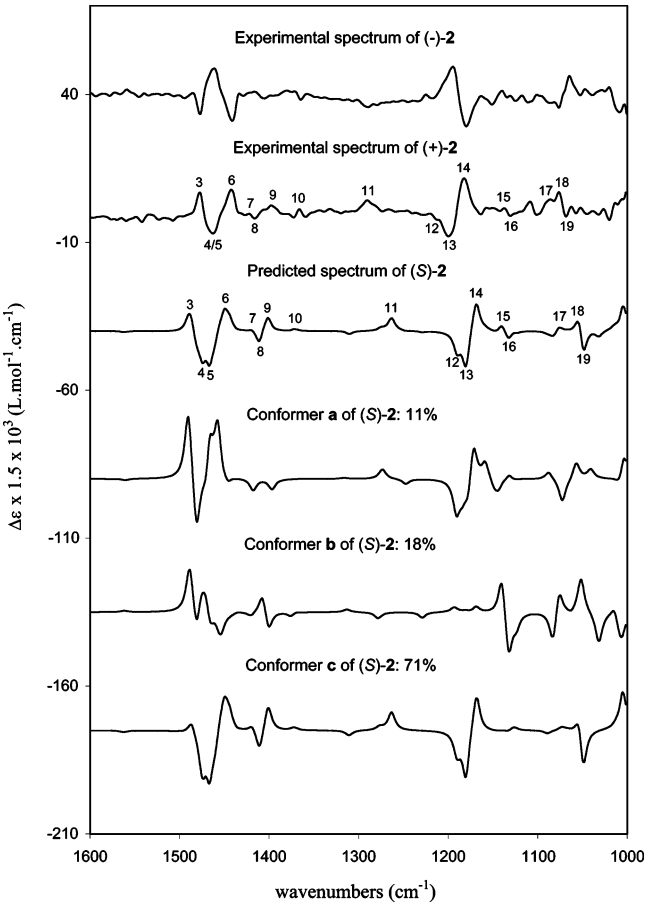

FIGURE 3. Comparison of the experimental VCD spectra of (−)-*tert*-butyl(dimethylamino)phenylphosphine−borane (−)-**2** and (+)-**2** at 0.26 M in CD_2Cl_2 solution (top two traces) with predicted VCD spectra (bottom three traces) of stable conformations of (*S*)-**2** (structure and conformation labels in Figure 1) obtained with the B3LYP/6-31+G(d) level. For predicted spectra, wavenumbers are scaled by the factor 0.9614. The trace labeled "predicted" (third from top) is the population-weighted spectrum with populations given in Table 1. Numbers indicate corresponding features in the predicted spectrum of (*S*)-**2** and the experimental spectrum of (+)-**2**.

CO_2 bands of the atmosphere, and relative weak intensities of the VCD signals of our samples which are a consequence of the conformational flexibility of the molecule (vide infra). Because of interferences from CD_2Cl_2 absorption, the region below 1000 cm^{-1} was not considered. According to previous works,[11−15] we thus focused our attention on the 1600−1000 cm^{-1} spectral range. The experimental IR spectrum in CD_2Cl_2 solution is shown in Figure 2, together with the spectrum of the equilibrium mixture of conformers which was obtained by weighting the spectrum of each conformer by its Boltzmann population. As delineated in Figure 2, convincing assignment of the fundamental transitions in the IR experimental spectrum can be made. The agreement is excellent for most of the signals (differences between predicted and observed frequencies are less than 8 cm^{-1}), with the exception of modes no. 7, 11, 17, and 18. The most notable differences concern the band (no. 17) at 1103 cm^{-1} in the experimental spectrum, which is shifted by 30 cm^{-1} and the band (no. 18) at 1068 cm^{-1}, which is relatively lower in intensity and broader than the corresponding band (1052−1054 cm^{-1}) in the computed spectrum.[27] Detailed comparison of the predicted frequencies to the experimental values and vibrational assignments are given in Table 2S of the Supporting Information. Most of the observed bands can be assigned to vibration modes of conformer **c** and support the conclusion that this species is predominant in solution. However, since the experimental spectrum shows a low intensity band (no. 14) at 1151 cm^{-1} corresponding to predicted absorption of conformer **b**, it can be concluded that this species is also present in solution in minor quantities, in agreement with theoretical predictions (**b**: 18%, Table 1).

The calculated VCD spectra of (*S*)-**2** are compared to the experimental VCD spectra of (+) and (−)-**2** in CD_2Cl_2 solutions in Figure 3. Despite low intensities of the VCD signals, the spectra of the enantiomers are nearly perfect mirror images, as one could expect. Agreement between the predicted population-weighted VCD spectrum of (*S*)-**2** and the recorded spectrum of (+)-**2** is good enough to support unambiguous elucidation of

(26) Measurements above 1800 cm^{-1} required the removal of the low-pass filter.

(27) These discrepancies should result from intrinsic limitations of the methods used to predicted spectra.[16,17]

the absolute configuration at the phosphorus atom. The assignment of fundamental modes is straightforward and agrees with the one done previously for IR spectra. The significant VCD bands in the experimental spectrum of (+)-**2** are a relatively intense positive−negative−positive triplet with peak maxima at 1476 (no. 3), 1462 (nos. 4,5), and 1441 cm^{-1} (no. 6), respectively, a positive band at 1289 cm^{-1} (no. 11), a relatively intense negative−negative−positive triplet at 1208 (no. 12), 1189 (no. 13), and 1181 cm^{-1} (no. 14), respectively, and finally, a positive−positive−negative triplet at 1085 (no. 17), 1075 (no. 18), and 1067 cm^{-1} (no. 19), respectively. The same characteristic features are clearly identified in the predicted VCD spectrum of (*S*)-**2**, except that the bands (no. 4) at 1475 cm^{-1} and (no. 5) at 1467 cm^{-1} are better resolved compared to the experimental spectra and that band no. 11 is shifted, as previously observed with IR spectra. The similarity of the signal shapes between the predicted and experimental spectra is also worth noting. In the 1500−1400 cm^{-1} and 1200−1100 cm^{-1} regions, the pattern of the predicted population-weighted VCD spectrum of (*S*)-**2** is significantly distinct from the one of major conformer **c** because of the superposition of intense bands from the spectra of minor species **a** and **b** (Figure 3). Indeed, the relative intensity of the positive peaks 3 and 6 is clearly affected by the contributions from the spectra of conformers **a** and **b**. Moreover, the positive-negative couplet 15−16 is absent from the spectrum of **c** and results from the population-weighted contribution of the spectrum of conformer **b**. Since the experimental VCD spectrum of (+)-**2** shows clearly these features, this confirms that conformer **b** is present in CD_2Cl_2 solution at a concentration similar to the population predicted by the DFT calculations. This is probably also the case for conformer **a**. However, since the expected solution concentration is lower, no definite conclusion can be derived from the spectra for this minor conformer. It should be noted that conformational flexibility of the molecule is detrimental to the signal intensity in the experimental VCD spectrum. In fact, averaging of the signals over the contributions of the three stable conformations of (*S*)-**2** leads to weaker band intensities in the population-weighted VCD spectrum compared to single conformer spectra, as shown in the 1500−1400 cm^{-1} and 1200−1100 cm^{-1} regions (Figure 3).[28]

Complementary energy calculations at different theoretical levels on the B3LYP/6-31+G(d) geometries were undertaken to compare with the above results (see Supporting Information). Extension of the basis set to 6-311+G(2d,2p) and use of a different functional (PBE1PBE/6-311+G(2d,2p)) induced only slight changes in the relative stabilities of the three conformers and the resulting populations (Table 1S). As previously, the predicted VCD spectra of (*S*)-*tert*-butyl(dimethylamino)phenylphosphine borane adduct match well the experimental spectrum of (+)-**2** (Figure 4S). In contrast, MP2/6-311+G(2d,-2p)//B3LYP/6-31+G(d) calculations predicted conformer **b** to be predominant over **c** and **a** (64, 30, and 6%, respectively). However, in this case, comparison between the experimental and the population-weighted predicted VCD spectra led to a much poorer agreement. This clearly indicates that the populations predicted using the MP2 energies do not reflect the distribution of the three conformers in equilibrium in the sample at 298 K, contrary to those calculated at the B3LYP level. Thus, despite the intrinsic limitations of the computational methods,

(28) Consequences of conformational flexibility for VCD studies in combination with DFT calculations have been recently discussed.[15j]

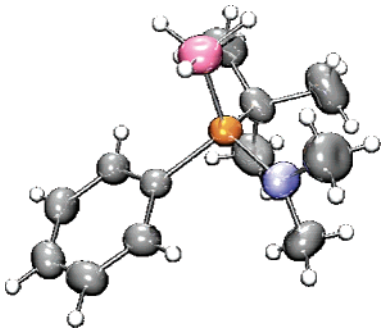

FIGURE 4. Thermal ellipsoidal view of (+)-(*S*)-*tert*-butyl(dimethylamino)phenylphosphine−borane. Ellipsoids are shown with 50% probability.

the small energy differences between the three conformers, and the low VCD signal intensities due to conformational flexibility, B3LYP/6-31+G(d) calculations seem to agree reasonably well with the experimental data and allow a conclusion on both the predominant conformation and the absolute configuration of the borane complex (+)-**2**.

The dextrorotatory enantiomer of *tert*-butyl(dimethylamino)-phenylphosphine−borane was crystallized from hexane, affording colorless crystals with a melting point of 53 °C (uncorrected). The X-ray crystal structure determination was carried out on a single crystal of (+)-**2** by anomalous dispersion and unequivocally revealed that the absolute configuration at the chirogenic phosphorus atom is *S*, as shown in Figure 4. This result fully confirms the assignment derived from VCD studies. The unit cell consists of four molecules in the same conformation. The structure of (+)−(*S*)-**2** in the crystalline phase exhibits geometrical parameters and characteristic torsion angles which are strikingly close to the values predicted by DFT calculations for conformer **c** (Figure 1, Table 1): the *tert*-butyl group presents a nearly staggered conformation, the phenyl ring is almost perpendicular to the P−B bond (C_7C_2PB = 82.6°) whereas the dimethylamino group is synclinal ($C_{14}NPB$ = −22.3°), and the nitrogen atom exhibits a flattened pyramidal shape ($C_{14}NPC_{13}$ = 161.1°). Thence, crystal packing does not have any notable influence on the molecular conformation, and the predominant conformer in solution and the structure in the crystalline phase of (+)−(*S*)-**2** are almost identical.[29]

Conclusions

Enantiomerically pure P-chirogenic aminophosphines are not easily accessible compounds. The procedure reported here offers straightforward access to the two enantiomers of *tert*-butyl-(dimethylamino)phenylphosphine protected by borane via expeditious resolution by semipreparative chiral HPLC. The absolute configuration *S* was unequivocally assigned to the dextrorotatory enantiomer (+)-**2** by comparison between predicted and experimental VCD spectra and independently confirmed by X-ray diffraction. The molecular structure of (+)−(*S*)-**2** in the crystal corresponds to the predominant conformer **c** in CD_2Cl_2 solution. Indications of the presence of minor proportions of less stable conformation **b** in the solution phase are found in IR and VCD spectra. As far as we can know, this is the first example of direct assignment of absolute configuration to a P-chirogenic aminophosphine.

(29) This result is in sharp contrast with recent findings by Polavarapu et al. in the case of (−)-(*S*)-*tert*-butylphenylphosphinoselenoic acid.[14]

Experimental Section

***tert*-Butyl(dimethylamino)phenylphosphine−Borane *rac*-2.** A solution of *tert*-butyl chloride (7.13 g, 8.45 mL, 77 mmol) in dry Et_2O (50 mL) was added slowly to Mg (1.82 g, 75 mmol) and dibromoethane (1%) in dry Et_2O (25 mL) under nitrogen. After the addition, stirring was continued for 4 h under reflux. The resulting gray suspension was then cooled in an ice bath, and a solution of $PPhCl_2$ (4.65 g, 3.50 mL, 26 mmol) in dry Et_2O (35 mL) was added dropwise. After 18 h at room temperature, the magnesium salts were filtered off under Ar to give a solution of *tert*-butylchlorophenylphosphine. Complete and clean reaction was observed by ^{31}P NMR spectroscopy of the crude mixture. ^{31}P NMR (81 MHz, C_6D_6): δ 121.9 (s). The resulting mixture containing *tert*-butylPhPCl was transferred by a syringe to a dropping funnel and was slowly added to a stirred solution of dimethylamine (7.03 g, 156 mmol) in dry Et_2O (150 mL) under Ar at −10 °C. After 12 h at room temperature, the solvent was partially evaporated under reduced pressure, and the ammonium salts were filtered off through Celite under Ar. The ^{31}P NMR (81 MHz, C_6D_6) spectrum of the resulting solution shows only one singlet at $\delta = 85.4$ ppm for the *tert*-butyl(dimethylamino)phenylphosphine **1**. BH_3-SMe_2 (2.27 g, 30 mmol) was added dropwise to a stirred and cooled solution at 0 °C of **1** in 130 mL of dry Et_2O. After 12 h at room temperature, evaporation of the solvent gave 3.9 g (67%) of the crude product. Flash chromatography on deactivated silica gel (10% NEt_3, AcOEt/light petroleum 1:20) afforded 1.8 g (8.07 mmol, 31%) of *tert*-butyl(dimethylamino)phenylphosphine−borane **2** as a colorless oil that solidified on standing in freezer. ^{31}P NMR (81 MHz, C_6D_6): δ 87.8 (q, $^1J_{PB} = 63.6$ Hz). ^1H NMR (200 MHz, C_6D_6): δ 0.81−2.25 (q, $^1J_{BH} = 95.4$ Hz, 3H), 1.12 (d, $^3J_{PH} = 13.5$ Hz, 9H), 2.44 (d, $^3J_{PH} = 8.4$ Hz, 6H), 7.04−7.08 (m, 3H), 7.62−7.71 (m, 2H). ^{13}C NMR (50 MHz, C_6D_6): δ 27.3 (d, $^2J_{PC} = 2.7$ Hz, 3C), 34.8 (d, $^1J_{PC} = 33.0$ Hz, 1C), 40.7 (d, $^2J_{PC} = 1.8$ Hz, 2C), 128.3 (d, $^2J_{PC} = 9.0$ Hz, 2C), 130.5 (d, $^4J_{PC} = 2.3$ Hz, 1C), 132.2 (d, $^1J_{PC} = 56.3$ Hz, 1C), 132.4 (d, $^3J_{PC} = 8.7$ Hz, 2C). IR (*c* 0.06 in CD_2Cl_2) (cm^{-1}): 3088, 3063, 2988−2808, 2391, 2349, 1487−1436, 1396, 1367, 1068, 989. TLC: R*f* = 0.22 (SiO_2, Et_2O). Anal. Calcd for $C_{12}H_{23}BNP$: C, 64.60; H, 10.39; N, 6.28. Found: C, 64.83; H, 10.31; N, 6.31.

Chromatographic Procedures. The analytical chiral HPLC experiments were performed on a screening unit composed of eleven chiral columns connected to a 12 positions valve, UV-detector, and on-line polarimeter. Hexane and propan-2-ol, HPLC grade, were degassed and filtered on a 0.45 μm membrane before use. The different analytical columns (250 × 4.6 mm) tested were Chiralcel OD-H, OJ-H, OC, OG, OB−H and Chiralpak AS and AD columns from Chiral Technology Europa (Illkirch, France), Whelk-O1 (S,S) and Ulmo (S,S) from Regis (Morton Grove, USA), Sumichiral OA-2500 from Sumitomo Chemicals (Osaka, Japan) and Kromasil CHI-TBB from Eka Nobel (Bohus, Sweden). Retention times Rt in minutes, retention factors $k_i = (Rt_i - Rt_0)/Rt_0$ and enantioselectivity factor $\alpha = k_2/k_1$ are reported. Rt_0 was determined by injection of tri-*tert*-butylbenzene. Analytical separation was performed on Chiralcel OJ-H (250 × 4.6 mm, 5 μm) in hexane/propan-2-ol (99/1) at 1 mL/min and 25 °C with UV detection 254 nm and polarimeter, Rt_1(-, *R*) = 9.33, Rt_2(+, *S*) = 11.15, k_1(-, *R*) = 2.01, k_2(+, *S*) = 2.60, $\alpha = 1.29$, Rs = 2.15. Semipreparative separation was performed on a typical HPLC unit including a valve with a 500 μL loop and a UV-detector. An amount of 500 μL of a 10 mg/mL solution of racemate was injected every 5 min on Chiralcel OJ (250 × 10 mm, 10 μm): flow-rate = 4.5 mL/min; mobile phase, hexane/propan-2-ol (99/1); detection on UV 254 nm, Rt_1(-, *R*) = 8.94, Rt_2(+, *S*) = 11. 56, k_1(-, *R*) = 1.80, k_2(+, *S*) = 2.62, $\alpha = 1.46$, Rs = 1.54. Twelve injections over 1 h afforded 30 mg of each enantiomers. $[\alpha]^{20}_D$ +29.3 ((+)-**2**, *c* 1.0 in toluene, ee > 99%), $[\alpha]^{20}_D$ −30.1 ((−)-**2**, *c* 1.0 in toluene, ee > 99%). The NMR and IR data of the two separated enantiomers were in perfect agreement with the data of the racemic compound.

Spectroscopic Measurements. IR and VCD spectra were recorded on a specific accessory coupled to a Fourier transform infrared spectrometer. A photoelastic modulator set at $^1/_4$ retardation was used to modulate the handedness of the circular polarized light. Demodulation was performed by a lock-in amplifier. An optical low-pass filter (<1800 cm^{-1}) put before the photoelastic modulator was used to enhance the signal/noise ratio. A transmission cell equipped with KBr windows and a 0.1 mm Teflon spacer was used. All solutions were prepared from a 4 mg sample in 70 μL of CD_2Cl_2. A VCD spectrum of the racemic mixture was subtracted from the VCD spectrum of the pure enantiomers. For the individual spectra of the enantiomers and racemic mixture, about 8800 scans were averaged at 4 cm^{-1} resolution (corresponding to 2 h measurement time). The spectra are presented without smoothing or further data processing.

Calculations. The fully optimized geometries, vibrational frequencies, IR, and VCD intensities for (*S*)-**2** were calculated using DFT with the B3LYP hybrid functional and the 6-31+G(d) basis set, using the Gaussian 03 program.[16] VCD intensities were calculated using the procedure of Cheeseman et al. implemented in the Gaussian 03 program.[17] IR and VCD spectra were simulated using Lorentzian band shapes, with full width at half-height γ = 5.0 cm^{-1}. The wavenumbers of predicted spectra were scaled by the factor 0.9614 suggested by Scott and Radom.[30]

Crystal and Molecular Structure of (+)-2. The X-ray data were collected at 293 K with graphite-monochromatized Mo Kα radiation. The compound (+)-**2** crystallizes in the orthorhombic system, in space group $P2_12_12_1$ with the unit cell consisting of four molecules. The lattice constants were refined by a least-squares fit of 3466 reflections in the θ range of 1.19−28.27° using standard procedures.[31] A total of 3436 observed reflections with $I > 0\sigma(I)$ were used to solve the structure by direct methods and to refine it by full matrix least-squares using F^2.[32] The final refinement converged to $R = 0.0389$ for 137 refined parameters and 3189 observed reflections with $I > 2\sigma(I)$. The absolute configuration at the chiral phosphorus atom was established as S_P. The absolute structure was determined by the Flack method with the final parameter $\chi = -0.02(9)$.[33] Cell refinement and data reduction were carried out with the Denzo and Scalepack computing package,[31] the structure solution SIR92,[34] and the structure refinement SHELXL-97.[32b]

We have deposited all crystallographic data for this structure in the Cambridge Crystallographic Data Centre under the number 273736.[35]

Acknowledgment. The financial supports by the CNRS and the MENESR (including a fellowship for J.-V.N.) are gratefully acknowledged. We are grateful to the CRC-MM (Fédération de Recherche des Sciences Chimiques de Marseille FR1739) and the National Computer Centre of Higher Education (CINES) for computer time. We thank Dr. Michel Giorgi and the Service Commun de Cristallochimie des Universités d'Aix-Marseille I & III for the crystallographic studies.

(30) Scott, A. P.; Radom, L. *J. Phys. Chem.* **1996**, *100*, 16502−16513.
(31) Otwinowski, Z.; Minor, W. *Macromolecular Crystallography, part A;* Carter, C. W., Jr., Sweet, R. M., Eds.; Methods in Enzymology, Vol. 276; Academic Press: San Diego, CA, 1997; pp 307−326.
(32) (a) Sheldrick, G. M.; Kruger, G. M.; Goddard, R. *Acta Crystallogr., Sect. A* **1990**, *46*, 467−473. (b) Sheldrick, G. M. *SHELXL97. Program for the refinement of crystal structures;* University of Göttingen: Göttingen, Germany, 1997.
(33) (a) Flack, H. D. *Acta Crystallogr., Sect. A.* **1983**, *39*, 876−881. (b) Flack, H. D.; Bernardinelli, G. *Acta Crystallogr., Sect. A.* **1999**, *55*, 908−915. (c) Flack, H. D.; Bernardinelli, G. *J. Appl. Crystallogr.* **2000**, *33*, 1143−1148.
(34) Altamore, A.; Cascarano, G.; Giacovazzo, C.; Guagliardi, A.; Burla, M. C.; Polidori, G.; Camalli, M. *J. Appl. Crystallogr.* **1994**, *27*, 435−436.
(35) University Chemical Laboratory, Cambridge Crystallographic Data Centre, 12 Union Road, Cambridge CB2 1EZ, UK.

Supporting Information Available: Computed energies and populations at different theoretical levels; calculated IR and VCD spectra for the three optimized conformations of (*S*)-*tert*-butyl-(dimethylamino)phenylphosphine−borane complex (*S*)-**2** and population-weighted spectra; experimental IR spectra of *rac*-**2** in CD_2Cl_2 solution; table with band positions and vibrational assignments; Cartesian coordinates for the three optimized conformations of (*S*)-**2** and two rotational transition states; table of crystal data, experimental details, crystal packing diagram, and crystallographic information file (CIF) for (+)-**2**. This material is available free of charge via the Internet at http://pubs.acs.org.

JO0605647